

# Effect of pumping parameters and composition of an active medium on the energy and efficiency of electric-discharge ArF and KrF lasers

C.N. Bagaev, A.M. Razhev, V.A. Chekavinskii,  
A.A. Zhupikov, and E.S. Kargapoltsev

*Institute of Laser Physics,  
Siberian Branch of the Russian Academy of Sciences, Novosibirsk*

Received October 7, 2001

The dependence of output energy and efficiency of the electric-discharge ArF (193 nm) and KrF (248 nm) excimer lasers on the geometry of active medium and parameters of a high-voltage excitation has been investigated. The design and parameters of the discharge chamber and of the high-voltage excitation circuit of the LC inverter type with automatic preionization (API) providing for the specific pump power of  $3.5 \text{ MW/cm}^3$  as high were developed and optimized. In a gas active mixture He:Ar:F<sub>2</sub> = 79.7:20:0.3 at the total pressure of 2.2 atm, we have managed to achieve, for the first time, the 850 mJ as high output energy of the ArF laser at the over-all efficiency of 1.7% and the pulse duration (FWHM) of  $15 \pm 1 \text{ ns}$ . For a KrF laser in the gas mixture of He:Ne:Kr:F<sub>2</sub> = 44.9:44.9:10:0.2 at the total pressure of 2.8 atm, the plug-in efficiency of 2.5% with output radiation energy of 840 mJ was achieved. The maximum output energy of the KrF laser was 1.15 J at the over-all efficiency of 2.2%, pulse duration (FWHM) of  $24 \pm 1 \text{ ns}$ , and the pulse power up to 48 MW.

## Introduction

The excimer electric-discharge ArF (193 nm) and KrF (248 nm) lasers are now widely used in microelectronics, photolithography, and medicine. For most of the technological applications, the important parameters of a laser are maximum achievable energy per pulse, the efficiency sufficiently high as compared to the stored energy, and the efficiency of a laser excitation circuit, as well as its operating costs. The operating costs are largely determined by the composition of the laser active medium. In this paper, we propose active media for excimer lasers based on He as a buffer gas; this requires studying the effect of pumping and active medium parameters on the energy and efficiency of ArF and KrF lasers.

To achieve high output energy (higher than 0.5 J) in the electric-discharge ArF and KrF lasers, investigators usually use rather complex excitation circuits operating at high discharge voltages and Ne as a buffer gas in active media.<sup>1-6</sup>

Reference 1 describes an excimer laser based on Ne and He as buffer gases. The output energies of 280 mJ (ArF) and 500 mJ (KrF) were obtained experimentally at the efficiency of 0.6 and 1.1%, respectively. The energy density in these experiments was  $2.4 \text{ J/l}$ , and the active medium of  $220 \text{ cm}^3$  volume was pumped at the charging voltages of 40–45 kV in the capacitor recharging circuit. The maximum output energy was reported in Ref. 2 to be 2 J for the ArF laser and 5 J for the KrF laser in Ref. 3. In both of these cases, Ne was used as a buffer gas. The medium was excited using a circuit with a two-stage Marx generator at the charging

voltages of 190–220 kV. The efficiency of both lasers did not exceed 0.5%.

In Ref. 4, Miyazaki et al. managed to obtain 1.3% efficiency in an ArF laser at the output energy of 295 mJ and the maximum output energy of 420 mJ at the efficiency of 1.1% in the gas mixture of Ne:He:Ar:F<sub>2</sub> = 59.4:35.6:4.9:0.1 at the pressure of 4 atm and the charging voltages of 28 and 36 kV, respectively. For the KrF laser, the maximum output energy of 600 mJ (efficiency of 1.3%) was obtained in a gas mixture Ne:Kr:F<sub>2</sub> = 98.6:1.3:0.09 at the pressure of 6 atm and the maximum efficiency of 2.8% (with the energy of 300 mJ) was obtained in the gas mixture of Ne:Kr:F<sub>2</sub> = 98.2:1.2:0.1 at the pressure of 4 atm. The laser with the active volume of  $116 \text{ cm}^3$  was excited using the circuit with capacitor recharging and automatic UV preionization at the charging voltages up to 36 kV. When studying the role of He and Ne buffer gases in the developed laser design, it was shown that lasing was not observed at all at the charging voltages of 30 kV and lower if only He was used as a buffer gas.

In Ref. 5 the efficiencies of 2.1 and 3.9% were obtained in Ne mixtures at the energy of 270 mJ (ArF) and 500 mJ (KrF), and in Ref. 6 the output energies of 500 mJ (ArF) and 810 mJ (KrF) were achieved at the efficiency of 1 and 2.6%, respectively. In these studies, the high-voltage excitation circuit with the capacitor recharging and automatic UV preionization was used. A TGI 1000/25 or TGI 2500/50V thyratrons was used as a switch.

The maximum values of the efficiency and the output energy in a helium-containing active medium for the ArF and KrF lasers were achieved in our previous

works (see Refs. 7 and 8). In Ref. 7 the following values were obtained: for the ArF laser the maximum efficiency was 1.5% (at the energy of 360 mJ) and the maximum output energy was 550 mJ (at the efficiency of 1.3%), and for the KrF laser the maximum efficiency was 2.4% (at the energy of 570 mJ) and the maximum output energy was 820 mJ (at the efficiency of 2.0%). To pump the active volume of 140 cm<sup>3</sup>, an LC-inverter circuit based on a standard RU-65 spark gap with automatic preionization of the medium was used as a source of excitation.

From the results obtained in Refs. 7 and 8 it is seen that the maximum output energy is achieved at the minimum efficiency and, vice versa, the maximum efficiency is achieved at the minimum output energy. This work continues our studies aimed at achieving the maximum values of the output energy and efficiency of excimer electric-discharge ArF and KrF lasers in active media based on He as a buffer gas. Therefore, the aim of this work was the experimental study of the power and time characteristics of pumping and lasing of gas-discharge ArF and KrF lasers, the study of design features of the discharge chamber, and optimization of the high-voltage LC-inverter type excitation circuit with a peaking capacitor and automatic UV preionization to achieve the high pump power providing for the maximum efficiency and output energy.

## Measurement technique and equipment

In our experiments, we measured power and amplitude-time characteristics of the voltage, current, and radiation pulses in a nanosecond time interval. We used an IMO-3N calorimeter to measure the radiation energy; the shape of a radiation pulse was recorded with a coaxial FEK-22 photoelement. The amplitude-time characteristics were measured using a Tektronix TDS 210 oscilloscope. Voltage pulses were studied with the use of capacitor and resistor dividers accurate to 2%. To measure parameters of current pulses, we have developed and made a low-inductance resistor shunt with the resistance of 0.02  $\Omega$ . The accuracy of voltage and current amplitudes measurements was 5% in all experiments.

## Experimental setup

The laser discharge chamber was made of caprolan, nickel electrodes of the laser had the cross section profile close to the Chang profile with the base width of 30 mm and the radii of the working and lateral surfaces of 100 and 13 mm. The separation between the electrodes was 27 mm, the length of the active part was 590 mm, and therefore the active volume at the 11-mm wide discharge was 175 cm<sup>3</sup>. Automatic UV preionization was initiated using two rows of 2-mm spark gaps. To improve the homogeneity of the UV preionization and to reduce the inductance of the high-voltage excitation circuit, 39 spark gaps were installed on each side of the high-voltage electrode at the distance of 10 mm from the electrode edge. The chamber ends were sealed by plane-

parallel MgF<sub>2</sub> plates, one of which served as an output mirror of the cavity. The second mirror of the cavity was an external dielectric mirror with the reflectance of 97% (193 nm) and 99% (248 nm). The cavity length was 120 cm. The gas mixture was blown across the discharge gap by a radial fan with the speed of 12 m/s; this provided the possibility of operating the laser at a pulse repetition frequency up to 50 Hz and higher. The total volume of the discharge chamber with the fan was roughly equal to 40 l.

To provide for high efficiency of energy transfer from the energy storage circuit to the peaking one and for high intensity of the energy deposition into the gas mixture, it was needed to design the high-voltage excitation circuit with the minimum possible inductance. Optimization of the operating conditions of this circuit involved selection of the best arrangement for the capacitors forming the capacitances  $C_1$  and  $C_2$  near the discharge chamber for achieving the maximum efficiency of the energy transfer. The developed high-voltage excitation circuit (Fig. 1) consisted of the storing  $C_1$  and  $2C_2$  capacitors and  $2C_3$  peaking capacitors. As a high-voltage switch, we used a standard RU-65 gas-filled spark gap. The  $C_1$  and  $2C_2$  capacitors were made as TDK UHV-6A (2.7 nF, 30 kV) capacitor banks consisting of 18 and 38 capacitors, respectively, and had the values of 48 and 102 nF; therefore the total charging capacitance was 150 nF. After the spark gap breakdown and alternation of the voltage polarity across  $C_1$ , the capacitors  $C_1$  and  $2C_2$  turned on in series and the charging capacitance was equal to 33 nF. The capacitances  $C_3$  were built up of TDK UHV-8A capacitors (1.3 nF, 40 kV), which were arranged directly on the both sides of the discharge chamber along it to achieve the maximum inductance of the discharge circuit. The inductance of the discharge circuit was 3.1 nH, the capacitance  $2C_3$  was 30 nF. The capacitor  $2C_3$  was charged from  $C_1$  and  $2C_2$  through 78 throttles, each having the inductance of 1  $\mu$ H and being connected to the UV preionization spark gaps to provide for synchronous operation. The total inductance of the throttles connected in parallel was 12.8 nH, the charging inductance  $L_1$  was 2.5  $\mu$ H.

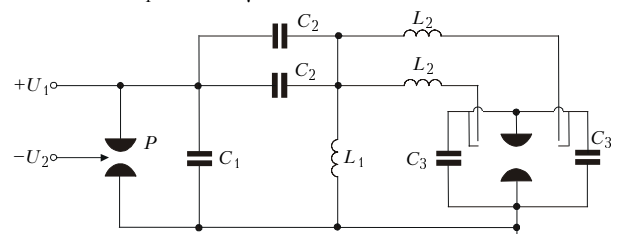


Fig. 1. Laser circuitry: RU-65 spark gap  $P$ ,  $C_1 = 48$  nF,  $C_2 = 51$  nF,  $C_3 = 15$  nF,  $L_1 = 2.5$   $\mu$ H,  $L_2 = 39 \times 1$   $\mu$ H.

## Results and discussion

### ArF laser

The parameters optimized in our experiments were the composition and the total pressure of the active gas

medium based on He as a buffer gas depending on the charging voltage. The optimal He:Ar:F<sub>2</sub> mixture ratio at the maximum output energy was 79.7:20:0.3. The optimal total pressure depended on the charging voltage and increased from 1.5 to 2.2 atm as the voltage varied from 19 to 26 kV.

Figure 2 depicts the oscillograms of voltage pulses across the discharge gap  $U$ , discharge current  $J$ , and the radiation pulse  $I_1$  for the ArF laser at the charging voltage of 26 kV. The measurements showed that the delay between the beginning of the main discharge current and the beginning of the UV preionization pulse was 100 ns. The duration (FWHM) of a current pulse was  $(25 \pm 1)$  ns. In this case, as is seen from the oscillograms of voltage  $U$  and current  $J$ , energy losses due to the oscillation process in the discharge circuit are low. The laser pulse  $I_1$  was delayed from the beginning of the current pulse by 20 ns and had the FWHM duration of  $(15 \pm 1)$  ns.

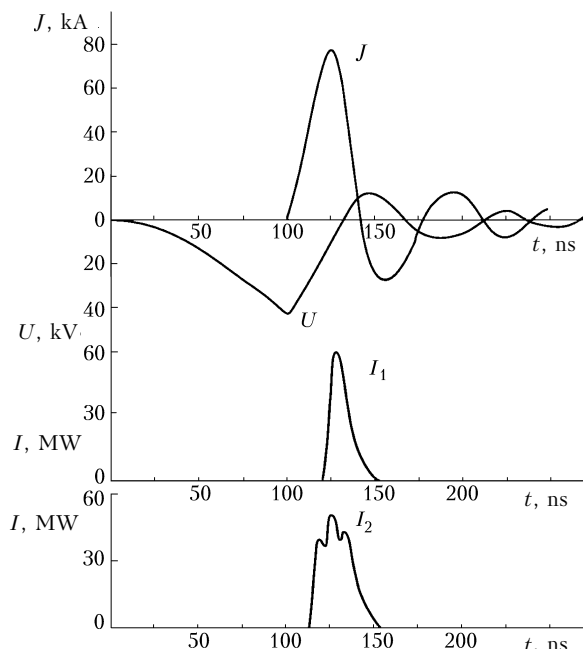


**Fig. 2.** Oscillograms of voltage pulses across the discharge gap  $U$ , discharge current  $J$ , laser pulses  $I_1$  (ArF laser) and  $I_2$  (KrF laser);  $U_0 = 26$  kV.

Figure 3 depicts the dependence of the voltage across the discharge gap  $U$  and the discharge current  $J$  on the charging voltage  $U_0$ . As the charging voltage  $U_0$  increases, the voltage  $U$  across the electrodes increases from 32 to 42 kV, whereas the discharge current  $J$  grows from 54 to 78 kA. To estimate the level of energy deposition into the discharge, we have calculated the mean pump power following the technique from Ref. 5. For this purpose, we have developed a program calculating the mean pump power from voltage and current oscillograms with the allowance for the inductive component of the voltage across the discharge gap. The dependence of the mean pump power  $P$  on the charging voltage  $U_0$  is shown in Fig. 3. It was finally

obtained that the mean pump power is equal to 2.1 MW/cm<sup>3</sup> in the active medium with He as the buffer gas at the minimum charging voltage of 19 kV. As the charging voltage increased, the mean power increased too and achieved 3.5 MW/cm<sup>3</sup> at 26 kV.

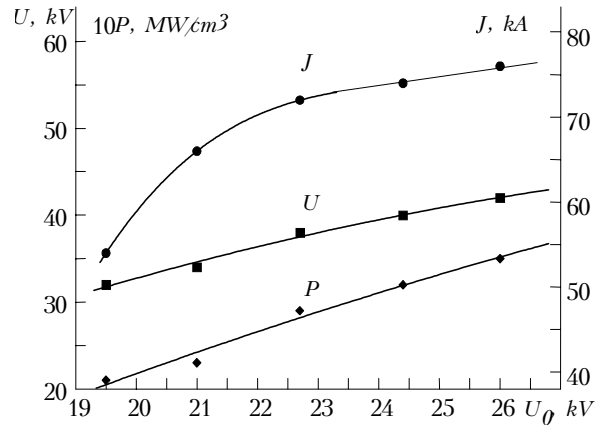


**Fig. 3.** Voltage across the discharge gap  $U$ , discharge current  $J$ , and the mean pump power  $P$  vs. charging voltage  $U_0$  in the mixture of He:Ar:F<sub>2</sub> = 79.7:20:0.3.

A subject of our study was the dependence of output energy  $E_1$  and the efficiency  $\eta_1$  of the ArF laser with the working mixture He:Ar:F<sub>2</sub> = 79.7:20:0.3 on the charging voltage  $U_0$ . The results of this study are depicted in Fig. 4. An important circumstance is the fact that the output energy increases with the growth of the charging voltage, as the efficiency does, and achieves the maximum value of 850 mJ with the efficiency of 1.7% at the maximum charging voltage of 26 kV. At the pulse duration of  $(15 \pm 1)$  ns the output power was 57 MW. A beam at the exit from the laser had a rectangular shape with the dimensions 27 × 11 mm.

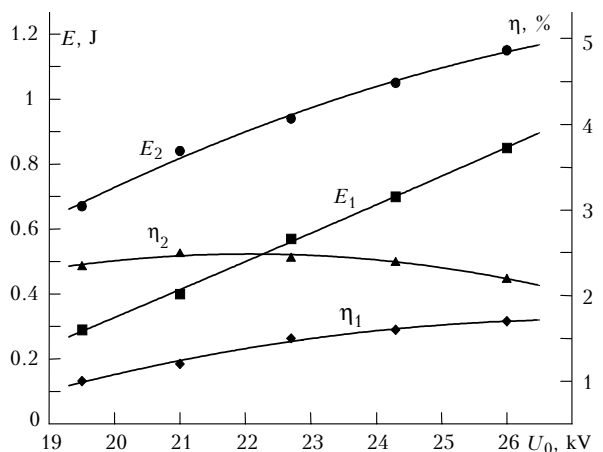


**Fig. 4.** Output energy and efficiency vs. charging voltage  $U_0$ : ( $E_1$ ,  $\eta_1$ ) for ArF laser (He:Ar:F<sub>2</sub> = 79.7:20:0.3) and ( $E_2$ ,  $\eta_2$ ) for KrF laser (He:Ne:Kr:F<sub>2</sub> = 49.9:49.9:10:0.2).

We have also studied the effect of buffer gas on the efficiency of an ArF laser. The experiments on measuring the output energy and efficiency of the ArF laser at different ratios of He and Ne content showed

that the addition of Ne as a buffer gas to He up to 50% did not change the laser output parameters, as well as the pulse oscillograms depicted in Fig. 2. The increase of the Ne content in the mixture over 50% and the transition to pure Ne as a buffer gas led to a 1.3 times decrease in the energy and efficiency of the ArF laser at the charging voltage of 26 kV.

### KrF laser

Using the experimental setup described above, we have studied the power and time characteristics of pumping and lasing in a KrF laser. As in the case with the ArF laser, the composition and the total pressure of the gas mixture were first optimized as functions of the charging voltage. The optimum ratio of the mixture components was measured at the maximum output energy. Unlike the ArF laser, addition of Ne to the laser active medium led to an increase in the output energy under the same pumping conditions. As a result, the optimum ratio of the mixture components He:Ne:Kr:F<sub>2</sub> was 44.9:44.9:10:0.2. The optimum total pressure depended on the charging voltage and varied from 2.6 to 3.1 atm as the voltage varied from 19 to 26 kV. The increase of the Ne content in the mixture over 50% and the transition to the pure Ne as a buffer gas led to an insignificant decrease in the energy and the efficiency.

For the KrF laser, the oscillograms of pulses and the dependence of the voltage across the discharge gap, discharge current, and mean pump power on the charging voltage are similar to those for the ArF laser and differ only in values. As the charging voltage increased from 18 to 26 kV, the voltage across the discharge gap grew from 28 to 40 kV, the discharge current increased from 51 to 78 kA, and the mean pump power in this case increased from 1.6 to 3.2 MW/cm<sup>3</sup>.

The output pulse  $I_2$  of the KrF laser (see Fig. 2) was delayed from the beginning of the current pulse by 16 ns and had the FWHM duration of (24±1) ns. The laser pulse had a structure consisting of three peaks coinciding in time with three path-tracings of radiation inside the cavity and connected with the changes in the medium gain not coinciding with the change of the pump pulse.

Figure 4 depicts the dependence of the output energy  $E_2$  and the overall efficiency  $\eta_2$  of the KrF laser with the working mixture He:Ne:Kr:F<sub>2</sub> = 44.9:44.9:10:0.2 on the charging voltage  $U_0$ . It can be seen that as the charging voltage increases, the efficiency increases up to the maximum value of 2.5% at the voltage of 21 kV. The output energy in this case was 840 mJ. As the charging voltage increased up to 26 kV, the efficiency gradually decreased down to 2.2%, and this allowed the output energy of 1.15 J to be achieved. This value corresponds to the pulse power of 48 MW.

According to Refs. 5 and 9, the decrease of the overall efficiency at the increasing charging voltage is connected with the excess over the pump intensity optimal for the KrF laser (about 2.5 MW/cm<sup>3</sup>). Comparing the results of this work and our previous work,<sup>8</sup> we can assume that further increase in the output energy at a high efficiency of the gas-discharge KrF laser can be achieved by increasing the laser active volume with the pump power keeping unchanged at the level of 2.5 MW/cm<sup>3</sup>.

### Conclusion

We have studied the dependence of the energy and efficiency of the electric-discharge excimer ArF and KrF lasers on the geometry of the active medium and parameters of the high-voltage excitation circuit. It has been shown that to obtain high output energy and efficiency, it is necessary to achieve high specific pump power. The discharge chamber and the LC-inverter type high-voltage excitation circuit with the UV preionization have been designed and their parameters have been optimized. These parameters allow the specific pump power of 3.5 MW/cm<sup>3</sup> as high to be obtained.

For the first time, the output energy of 850 mJ at the efficiency of 1.7% has been achieved in an ArF laser with He as the buffer gas. The FWHM duration of the pulse was (15±1) ns, and the pulse power in this case was 57 MW.

For the KrF laser in the active medium He:Ne:Kr:F<sub>2</sub> = 44.9:44.9:10:0.2 at the total pressure of 2.8 atm, the overall efficiency of 2.5% has been obtained at the output energy of 840 mJ. The maximum output energy of the KrF laser (1.15 J) has been achieved with the efficiency of 2.2% at the FWHM pulse duration of (24±1) ns and the pulse power of 48 MW.

### References

1. E. Armandillo, F. Bonanni, and G. Grasso, *Opt. Commun.* **42**, No. 1, 63–66 (1982).
2. I.E. Andrew, P.E. Dyer, and P.I. Roebuck, *Opt. Commun.* **49**, No. 3, 189–194 (1984).
3. S. Watanabe and A. Endoh, *Appl. Phys. Lett.* **41**, No. 9, 799–801 (1982).
4. K. Miyazaki, T. Hasama, K. Yamada, T. Fukatsu, T. Eura, and T. Sato, *J. Appl. Phys.* **60**, No. 8, 2721–2728 (1986).
5. V.M. Borisov, I.E. Bragin, A.Yu. Vinokhodov, and V.A. Vodchits, *Kvant. Elektron.* **22**, No. 6, 533–536 (1995).
6. V.M. Borisov, A.V. Borisov, I.E. Bragin, and A.Yu. Vinokhodov, *Kvant. Elektron.* **22**, No. 5, 446–450 (1995).
7. A.A. Zhupikov and A.M. Razhev, *Kvant. Elektron.* **24**, No. 8, 683–687 (1997).
8. A.A. Zhupikov and A.M. Razhev, *Kvant. Elektron.* **25**, No. 8, 687–689 (1998).
9. V.M. Borisov, F.I. Vysikailo, E.G. Ivanova, and O.B. Khristoforov, *Kvant. Elektron.* **12**, No. 6, 1196–1203 (1985).